World Scientific
www.worldscientific.com

COMPUTATIONAL DESIGN FOR MULTIFUNCTIONAL MICROSTRUCTURAL COMPOSITES

YUHANG CHEN, SHIWEI ZHOU, QING LI[*]

*School of Aerospace, Mechanical and Mechatronic Engineering, University of Sydney,
Sydney, NSW 2006, Australia*
[*]Q.Li@usyd.edu.au

As an important class of natural and engineered materials, periodic microstructural composites have drawn substantial attention from the material research community for their excellent flexibility in tailoring various desirable physical behaviors. To develop periodic cellular composites for multifunctional applications, this paper presents a unified design framework for combining stiffness and a range of physical properties governed by quasi-harmonic partial differential equations. A multiphase microstructural configuration is sought within a periodic base-cell design domain using topology optimization. To deal with conflicting properties, e.g. conductivity/permeability versus bulk modulus, the optimum is sought in a Pareto sense. Illustrative examples demonstrate the capability of the presented procedure for the design of multiphysical composites and tissue scaffolds.

Keywords: Topology optimization; homogenization; multifunctional; periodic composite; scaffold tissue engineering; cellular materials.

1. Introduction

As innovative technologies rapidly emerge, multifunctional demands are increasingly placed on the material systems involved. However, the development of novel engineered materials for an array of desirable physical properties is rather challenging and often involves a laborious trial-and-error process in material design and characterization, making empirical or experiment-based methods sometimes uneconomic (if not infeasible). Periodic microstructural composites have gained substantial attention for their advantages in design and fabrication, signifying a class of promising multifunctional cellular materials. In this respect, computational modeling has become a major alternative to experimental methods for developing new materials, where finite element based homogenization and its inverse form exhibit special promise.

Pioneered by Sigmund, the inverse homogenization method[1] aims to achieve specific physical properties by tailoring the microstructural configuration of a representative volume element (RVE) or periodic base cell (PBC). The idea is to minimize the

---

[*]Corresponding author.

difference between the target and homogenized properties within a topology optimization framework. Over the last decade, considerable efforts have been devoted to this area with a special focus on various individual physical properties[2], including extremal bulk/shear modulus, negative Poisson's ratio, conductivity and permeability. Although some studies consider the design of competing material properties, e.g. thermal and electrical conductivities[3,4], stiffness and conductivity[5,6] and stiffness and permeability[7], few specifically address the mathematical equivalence for quasi-harmonic fields[8,9]. This paper presents a unified inverse homogenization procedure incorporating the aforementioned physical properties and their combinations with the elasticity tensor to design multifunctional composites for engineering applications.

2. Materials and Methods

For many steady state scalar fields, as summarized in Table 1, the governing equation commonly takes the following quasi-harmonic form[9]

$$\text{div}(\kappa \nabla \phi) + Q = 0 \tag{1}$$

where ϕ denotes the known scalar function and κ the media properties. It is noted that for vector fields of the elastostatic problem, the equilibrium equation, $\text{div}(C : \varepsilon(u)) + b = 0$, takes a similar form to the quasi-harmonic Eq. (1).

Table 1. Steady state scalar fields governed by the quasi-harmonic equation.

Scalar field	Unknown(ϕ)	Coefficient (κ)	Constant (Q)
Heat transfer	Temperature	Thermal conductivity	Internal heat source
Incompressible flow	Stream function	Unity	Twice the vorticity
Incompressible flow	Velocity potential	Unity	Zero
Gas Diffusion	Concentration	Diffusivity	Zero
Elastic torsion	Stress function	(Shear modulus)$^{-1}$	Twice the rate of twist
Seepage flow	Hydraulic head	Permeability	Zero
Electric conduction	Voltage	Electric conductivity	Zero
Electrostatics	Permittivity	Charge density	Zero
Magnetostatics	Magnetic potential	Reluctivity	Charge density
Incompressible lubrication	Pressure	(Film thickness)^3/viscosity	Lubricant supply
Linear elastostatics	Displacement (u)	Elasticity tensor (C)	Force (b)

The homogenization method has proven effective for calculating the effective properties of a PBC with given composition and configuration. Based upon the asymptotic expansion and periodicity assumption[2], the homogenization procedure calculates the effective elasticity tensor within the finite element framework as

$$C_{ijkl}^H = \frac{1}{|\Omega|} \sum_{e=1}^{NE} ((u_0^e(\varepsilon^{0(ij)}) - u^e(\varepsilon^{*(ij)}))^T C_s^e(\rho^e)(u_0^e(\varepsilon^{0(kl)}) - u^e(\varepsilon^{*(kl)}))). \tag{2}$$

where Ω denotes the total volume of the design domain, C_{ijkl}^{H} the homogenized elasticity tensor and C_{s}^{e} the elemental elasticity tensor interpolated by empirical formula, e.g. solid isotropic material with penalization (SIMP) method[10]. $u_{0}^{e}(\varepsilon^{0(ij)})$ and $u^{e}(\varepsilon^{*(ij)})$ are the nodal displacements induced by the unit test strain $\varepsilon^{0(ij)}$ and fluctuation strain $\varepsilon^{*(ij)}$, respectively[2,5].

Similarly, the effective properties of a quasi-harmonic field can be computed as[11]

$$ K_{ij}^{H} = \frac{1}{|\Omega|}\sum_{e=1}^{NE}\kappa_{c}^{e}(\rho^{e})\cdot(I-\frac{\partial\chi_{i}}{\partial y_{j}}) . \tag{3}$$

where K_{ij}^{H} and κ_{c}^{e} are the homogenized and local elemental property tensors, respectively, and χ_{i} is a solution to the following characteristic equation, similar to Eq. (1)[5]

$$ \frac{\partial}{\partial x_{i}}\left(\kappa\frac{\partial\chi}{\partial x_{j}}\right)=\frac{\partial\kappa}{\partial x_{i}} . \tag{4}$$

Conversely, the inverse homogenization aims to tailor PBC configuration for one or more specific (or extremal) physical properties[1,2]. It is often formulated to either maximize objective properties or minimize the squared difference between the target (normally on the material bounds) and homogenized values[5,11].

Having defined the effective properties for vector (Eq. (2)) and scalar (Eq. (3)) fields, the design of multifunctional microstructural materials can be formulated as a topology optimization problem given by

$$ \begin{cases} \min J = \sum_{r=1}^{M} w_{r}f_{r} \\ s.t. \int_{\Omega}\rho\,d\Omega=V \end{cases} \tag{5}$$

where the weights satisfy $\Sigma w_{r}=1$, f_{r} denotes the rth normalized objective property, M the number of properties involved, and V the volume constraint. By varying the weights, one can obtain a series of solutions, thereby determining a Pareto front for competing properties. To solve the topology optimization in Eq. (5) and avoid checkerboarding, the method of moving asymptotes (MMA)[12] and a filter technique[13] are adopted herein.

3. Results and Discussion

Although the methodology described in this paper allows us to design microstructural materials for any meaningful and sensible physical properties, given in Table 1, and their combinations, we will restrict our attention to heat/electrical conductivity, fluid permeability and their combination with the stiffness objectives for demonstrative purposes. It is noted that the same homogenization (Eq. (3)) and sensitivity equations[5,11] can be applied for both conductivity and permeability designs due to their mathematical equivalence, given by Eq. (1), making the numerical procedure established here more versatile.

Owing to the cubic symmetry in 3D, 1/8 of the PBC is discretized into 20×20×20 8-node elements with symmetric and periodic boundary conditions in the following examples.
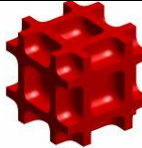
3.1. *Composite design for maximum bulk modulus and conductivity*

As one of the most typical engineered materials, thermal or electrical conductors with a degree of mechanical stiffness are of particular interest. It is assumed that the high stiffness material has a low conductivity (i.e. E_1=20 and k_1=1, in red/dark color in the color /black and white pictures below), while the high conductivity material has a low stiffness (i.e. E_2=1 and k_2=20, in green/light color)[5,6]. This example generates a Pareto optimum for the competing properties of bulk modulus C_b and conductivity K_c by formulating the design problem as

$$\min J = w_b f_b + w_c f_c = w_b C_b^{-1} + w_c K_c^{-1}. \tag{6}$$

To deal with intermediate properties during the design, three different schemes, namely arithmetic and Hashin-Shtrikman (H-S) upper and lower bounds[11], are considered for conductivity, but only the arithmetic bound (i.e. $E(\rho)=\rho^p E_1+(1-\rho)^p E_2$, p=3) for the Young's modulus[2]. It should be pointed out that the material interpolation schemes affect the final results. Table 2 summarizes these effects on the resultant PBC configurations for the fully-conductive (w_b=0; w_c=1) and fully-stiff (w_b=1; w_c=0) designs in separate phases. It is observed that as a benchmark problem, the stiffer material forms the matrix to maximize the bulk modulus in the fully-stiff design; while the conductive material forms the matrix in the fully-conductive design. In both cases, the opposite phase is developed as an inclusion to minimize its influence on the overall objective.

Table 2. Effects of interpolation schemes on design of base cell (2×2×2).

	Full conductivity (Arithmetic)	Full conductivity (H-S upper)	Full conductivity (H-S lower)	Full stiffness (Arithmetic)
Phase I (E_1=20, k_1=1)				
Phase II (E_2=1, k_2=20,)				
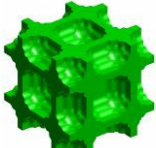
By varying one of the weights in Eq. (6), from 0 to 1, a series of topologies are obtained for different conductivities and bulk moduli. Figure 1 plots the Pareto fronts in the normalized function space for these three different interpolation schemes. All these

three curves are consistently convex, demonstrating the effectiveness of using the linear weighting formulation, (Eq. (6)), for solving the multifunctional optimization problem. From this example, it appears that the arithmetic interpolation provides the best Pareto optimum.
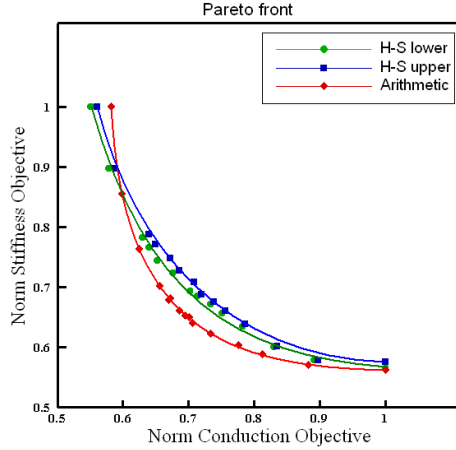

Fig. 1. Pareto fronts for bi-objective designs with different material interpolation schemes.

3.2. *Scaffold design for the specific stiffness tensor and maximum permeability*

The design and fabrication of porous biomaterials has been a key to the success of scaffold tissue engineering. A scaffold must provide certain stiffness to support *in-vivo* implantation and high permeability to maximize nutrient delivery and metabolite removal. This example applies inverse homogenization to the design of periodic scaffolds.

To determine the stiffness target, two samples of bone tissue, namely human iliac crest (HIC) bone (75% porosity) and mini-pig trabecular (MTR) bone (49% porosity)[14] are exploited herein. As per the previous example, solid and void materials represent the scaffold ($E_1=E_{scaffold}$) and tissue hydrolysate ($E_{tissue}=10^{-3}E_1$), respectively. The objective function is formulated in terms of the difference between the homogenized (C^H) and target stiffness (C^*) tensors as well as the maximization of the permeability tensor K_p as,

$$\min J = w_s f_s + w_p f_p = w_s [C^H - C^*]^2 + w_p K_p^{-1}. \qquad (7)$$
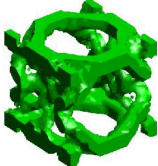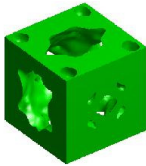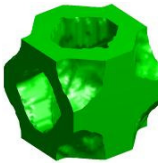
where w_s and w_p are weighting factors, which in this formulation also contain the normalization of individual objective components. Considering properties of general biomaterials, a Young's modulus of $E_{scaffold}=6\text{GPa}$[14,15] is adopted for the scaffold design.

Table 3 summarizes the design results. It is clear that there is good overall agreement between the target and effective stiffness tensors in all the design cases. Inclusion of the permeable criterion in Eq. (7) improves the overall permeability by over 10% for both the HIC scaffold and MTR scaffold in Table 3. In particular, in the lower porosity MTR case, excluding the permeability criterion leads to a blind channel in the vertical direction, rendering the scaffold non-functional in this course.

4. Concluding Remarks

Many physical problems can be described by either vector or scalar fields that are commonly governed by analogical partial differential equations. To develop novel periodic cellular materials with such fields, a unified design framework is presented to seek desirable physical properties. A multiobjective topology optimization is formulated

Table 3. Two different scaffold designs with or without permeability criterion.

	HIC	HIC (w_p=0)	MTR	MTR (w_p=0)
Base cell topology for scaffold				
Porosity	75.5%	75.0%	50.6%	50.0%
$E_{11}/E_{11Target}$	409.8793/410	409.1434/410	1061.15/1050	1050.10/1050
$E_{22}/E_{22Target}$	289.9245/289	289.9633/289	2020.34/2025	2026.11/2025
$E_{33}/E_{33Target}$	155.5836/155	155.1509/155	2072.45/2050	2051.18/2050
$G_{13}/G_{13Target}$	74.1289/75	73.4130/75	652.29/750	744.14/750
$G_{23}/G_{23Target}$	89.7344/90	89.7777/90	327.54/500	497.34/500
$G_{12}/G_{12Target}$	124.7524/125	124.6076/125	293.22/500	499.96/500
Permeability	65.1823	58.7146	45.9645	40.6237

to solve such cellular material design problems. Two examples are presented: the first seeks a Pareto optimum for the two competing properties of bulk modulus and conductivity, and the second devises scaffolds for load-bearing tissue engineering with targeted stiffness and maximum permeability. Both examples demonstrate the capability of the proposed unified design framework. It is noted that all these designed PBC composites can be materialized using free-form fabrication methods[14,15].

Acknowledgment

References

1. O. Sigmund, *Int. J. Solids Struct.* **31**, 2313-2329 (1994).
2. M. Bendsøe, O. Sigmund, *Topology Optimization: Theory, Method and Applications* (Springer, Berlin, 2003).
3. S. Torquato, S. Hyun, and A. Donev, *J. App. Phy.* **94**: 5748-5755 (2003).
4. S. Torquato, S. Hyun, and A. Donev, *Phys. Rev. Lett.* **89**, ARTN 266601 (2002).
5. N. de Kruijf, S. Zhou, Q. Li, Y. Mai, *Int. J. Solids Struct.* **44**, 7092-7109 (2007).
6. V. Challis, A. Roberts, A. Wilkins, *Int. J. Solids Struct.* **45**, 4130-4146 (2008).

7. J. Guest and J. Prévost, *Int. J. Solids Struct.* **43**, 7028-7047 (2006).
8. G. Steven, Q. Li, Y. Xie, *Comput. Mech.* **26**, 129-139 (2000).
9. A. Sommerfeld, *Partial Differential Equations in Physics* (Academic Press, New York, 1949).
10. M. Bendsøe, *Struct. Optim.* **1**, 193-202 (1989).
11. S. Zhou, Q. Li, *J. Phys. D: Appl. Phys.* **40**, 6083-6093 (2007).
12. K. Svanberg, *Int. J. Numer. Methods Eng.* **24**, 359-373 (1987).
13. O. Sigmund, *Mech. Struct. Mach.* **25**, 495-526 (1997).
14. C. Lin, N. Kikuchi, S. Hollister, *J. Biomech.* **37**, 623-636 (2004).
15. S. Hollister, *Nat. Mater.* **4**, 518-524 (2005).